The Conformational Behaviour of Fucosyl and Carbafucosyl Mimetics in the Free and in the Protein-Bound States

Mercedes Carpintero,[a] Alfonso Fernández-Mayoralas,[a] and Jesús Jiménez-Barbero*[a]

Keywords: Carbasugars / Conformational analysis / Glycomimetics / Molecular mechanics / NMR spectroscopy

The conformational behaviours of fucosyl glycosides bearing a glyceryl aglycon and their corresponding carbafucosyl glycomimetics have been studied both in aqueous solution and when bound to a fucose-specific lectin (*Aurelia Aurantia Agglutinnin*), using a combination of NMR spectroscopy (*J* and NOE data) and molecular mechanics calculations. Analogies and differences between the mimetics and the natural compounds have been found.

Introduction

The quest for inhibitors of glycosidase and glycosyl transferase, as well as for stable glycomimetics, has furnished different groups of oligosaccharide analogues, with the glycosidic and endocyclic oxygen atoms substituted by other atoms.[1] Thus, carbon-, thio- and imino-linked glycosides, carbasugars and other derivatives have been employed, with different degrees of success.[2,3] For these pseudosaccharides to be biologically useful, one probable requirement is that their conformational behaviour should be analogous to that of the natural compound, in order to minimize the entropic costs of the recognition process with the receptor.[4] It should be stressed that, in principle, the substitution of the *exo*- or *endo*-cyclic oxygen atoms by other atoms should result in a change in the size and/or the electronic properties of the glycosidic linkage, particularly in the anomeric effects.[5] Therefore, it is appropriate to determine how the three-dimensional structures of the synthetically prepared derivatives are affected by such modifications, in comparison with those of the glycosides. In this context, we have recently reported that for the *C*-glycosyl, *S*-glycosyl and carba analogues of lactose,[6] in the absence of the stereoelectronic stabilisation due to the anomeric effect, conformations that are not consistent with the *exo*-anomeric-*syn* disposition might be adopted (between 4−50%), depending on the strength of 1,3-type *syn*-diaxial interactions and the particular bond length and angle values. Regarding recognition of these analogues by proteins and enzymes, we have also reported that thiocellobiose is bound by β-glucosidase from Streptomyces Sp. in the conformation usually found for regular *O*-glycosides (*syn*-Φ,Ψ).[7] However, we also reported that the *C*-glycosyl analogue of lactose is bound by *E. coli* β-galactosidase in an unusual, high-energy conformation.[8] Moreover, this derivative, C-lactose, is recognised by two lectins − namely, ricin-B[9] and galectin-1[10] − in other distinct conformations. In particular, ricin-B selects the *anti*-Ψ conformation, while galectin-1 binds the *syn*-Ψ minimum, the recognised minimum for peanut agglutinnin as described by Kishi's group.[11] These results have prompted us to extend our studies to determine the degree of similarity between other sugars and other saccharide analogues with different glycosidic linkages, in the free and in the protein-bound states.[12] In this context, we report here on a conformational study of two carba analogues of α-L-fucose, using a combination of NMR spectroscopy and molecular mechanics calculations.[13] The bioactive conformations of these glycomimetics and of their corresponding glycosyl compounds when bound to a fucose-binding lectin, *Aurelia Aurantia Agglutinin*, have also been derived.[14]

[a] Instituto de Química Orgánica, CSIC,
Juan de la Cierva 3, 28006 Madrid, Spain
Fax: (internat.) + 34-91/564-4853
E-mail: iqoj101@iqog.csic.es

Results and Discussion

Synthesis

The glyceryl fucopyranosides **1** and **2** were prepared by glycosylation of fucopyranosyl bromide **6**, prepared in situ from ethyl 3,4,6-tri-*O*-benzyl-1-thio-α-L-fucopyranoside (**5**), with D- and L-glycerol derivatives **7** and **8**, respectively, using the so-called halide ion catalysed glycosidation (Scheme 1).[15] Thus, treatment of **6** and **7** in the presence of Bu_4NBr stereoselectively gave the α-glycoside **9**, although in low yield (39% from **5**). A number of by-products derived from bromide **6** were also observed. Hydrogenation of **9** in the presence of trifluoroacetic acid resulted in the cleavage of the benzyl and isopropylidene groups, affording the unprotected glycoside **1** in excellent yield (99%). The same synthetic scheme applied to the alcohol **8** gave the fucopyranoside **2**.

The pseudofucopyranosides **3** and **4** were prepared by alkylation of the common intermediate **11**[16] with tosylates **14** and **15**, giving **12** and **13** in 70 and 73% yields, respectively (Scheme 2). Cleavage of the acetals by acid hydrolysis, followed by hydrogenolysis of the benzyl group, furnished the targets **3** and **4** (Figure 1).

  1434−193X/01/0204−0681 $ 17.50+.50/0

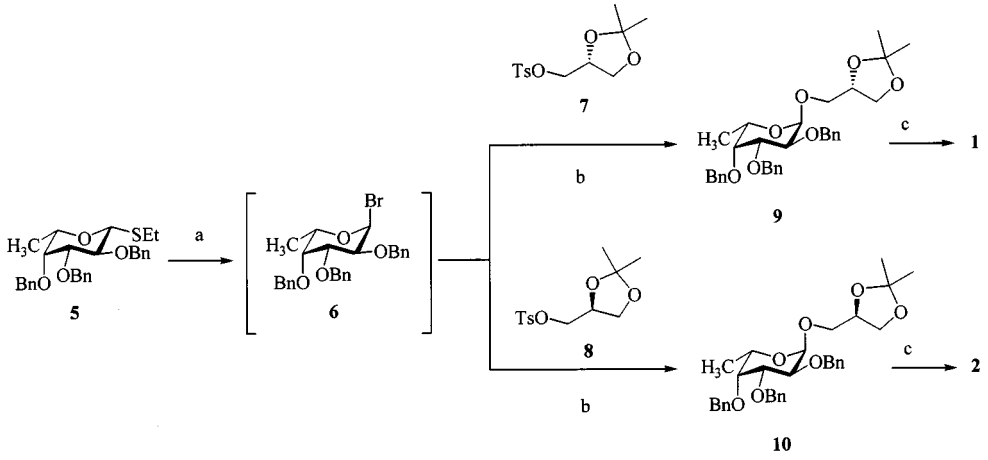

Scheme 1. Reagents and conditions: (a) Br_2, CH_2Cl_2, 0 °C, 2 h; (b) Bu_4NBr, DMF, room temp., 2 h, 39% for **9** and 47% for **10** (2 steps); (c) H_2, Pd/C, CF_3CO_2H, MeOH, room temp., 24 h, 99%

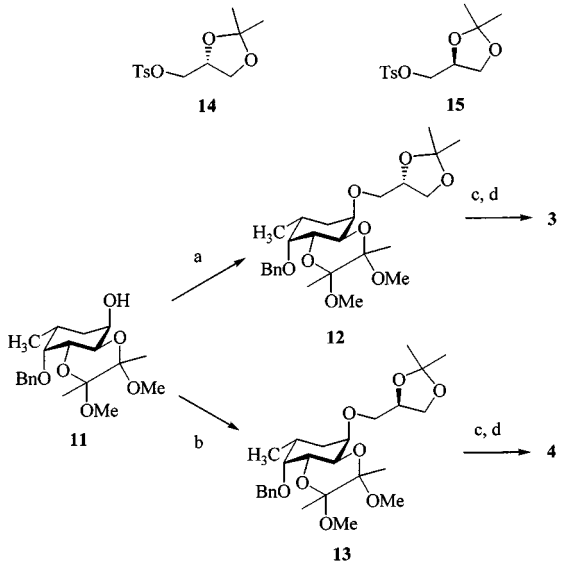

Scheme 2. Reagents and conditions: (a) NaH, DMF, Bu_4NI, **14**, 90 °C, 20 h, 70%; (b) NaH, DMF, Bu_4NI, **15**, 90 °C, 20 h, 73%; (c) AcOH/H_2O (2:1), 100°C, 2 h; (d) Pd/C, H_2, MeOH, room temp., 2 h, 52% for **3** and 58% for **4** (2 steps)

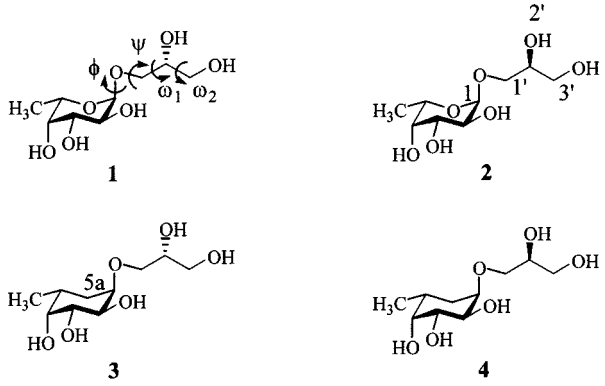

Figure 1. Schematic representation of compounds **1**–**4**, showing the torsion angles

Molecular Mechanics and Dynamics Calculations

These compounds show three torsional degrees of freedom for their glycosidic and aglyconic linkage, and therefore they resemble a (1→6)-linked saccharide molecule.[17] Therefore, in the first step, the populations of the different staggered rotamers around the φ/Ψ/ω1/ω2 linkages were estimated (Figure 1) by using the MM3* force field.[18] Glycosidic torsion angles are defined thus: Φ as H1′–C1′–O–C1, Ψ as C1′–O–C1–C2, and ω1 as O–C1–C2–C3 and ω2 as C1–C2–C3–O3. The results are shown in Table 1.

Table 1. Steric energy values [kJ/mol] (MM3*) for the minima of compounds **1**–**4**; the global minima are in bold; Ψ values correspond to *anti* minima

Conformation ($\omega_1\omega_2$)	Energy [kJ/mol] **1**	**2**	**3** (*R*)		**4** (*S*)	
			Φ *exo*	Φ non-*exo*	Φ *exo*	Φ non-*exo*
g−g−	66.8	68.3	100.3	94.6	91.2	95.2
g−g+	**64.6**	73.4	**89.9**	92.3	96.2	100.3
g−a	69.7	74.2	92.7	97.4	97.0	100.7
g+g−	70.9	**67.2**	94.0	98.7	**90.3**	94.3
g+g+	67.2	70.4	90.1	94.8	93.5	97.4
g+a	71.6	73.1	94.5	99.6	96.2	100.3
ag−	73.1	71.2	96.0	99.3	94.3	96.7
ag+	71.2	73.8	94.1	97.8	96.6	97.2
aa	76.5	77.1	99.3	102.9	100.3	103.3

For Ψ and ω, the rotamers are defined as g+ (60°), g− (−60°), and *anti* (180°), while for Φ, conformers conforming to the *exo* anomeric orientation (Φ ca. +60) and those not conforming (Φ ca. −60) are denoted as *exo* and non-*exo*, respectively. From these energy values, probability distributions were obtained according to a Boltzmann function (Table 2). For the regular glycosides, *anti* and non-*exo* conformers around Φ were not local minima: they converged in all cases to *exo*-oriented conformers. For the torsional Φ/Ψ/ω combinations, a major conformation (> 40%) is always predicted, its features depending on the stereochemistry at the glycerol side chain. Two additional conformations above 10%, defined in both cases as g-g− and g+g+ for ω1/ω2, are also predicted (Table 2). With the carba analogues, in contrast, conformers displaying the non-*exo* orientation around Φ are predicted to occur in a

Table 2. Population distributions for the minima of compounds **1−4**; the global minima are in bold; Ψ values correspond to *anti* minima

Conformation ($\omega_1\omega_2$)	Population (%)					
	1	**2**	**3**		**4**	
			exo	non-*exo*	*exo*	non-*exo*
g−g−	16.3	26.1	0.0	4.1	22.4	4.1
g−g+	**51.0**	3.4	**27.5**	**9.9**	2.9	0.6
g−a	6.6	2.5	9.1	1.4	2.2	0.6
g+g−	4.1	**40.8**	5.2	0.8	**31.9**	**6.4**
g+g+	13.1	11.3	25.3	3.6	8.9	1.9
g+a	3.1	3.8	4.4	0.0	2.9	0.6
ag−	1.7	8.2	2.5	0.0	6.4	2.6
ag+	3.6	2.9	5.2	1.1	2.6	1.9
aa	0.4	0.8	0.0	0.0	0.6	0.3

proportion of about 20%. Two major orientations around ω1 and ω2 are also found (Figure 2). Regarding Ψ, values close to the *anti* orientation were essentially found in all cases.

Additional information on the conformational stability of the different minima was obtained from MD simulations with the MM3* force field, using the GB/SA (Generalized Born solvent-accessible surface area) continuum solvent model for water.[19] Independently of the starting minimum, the calculated trajectories showed several interconversions among the different regions, and displayed a clear resemblance to the conformer populations described above. In particular, only *exo*-anomeric conformers were predicted for the glycosides, while minor excursions to non-*exo*-anomeric regions were detected for both carbaglycosyl compounds (data not shown). The Ψ angle was always close to 180°. Interconversions around ω1 and ω2 were very frequently found for all compounds, in agreement with the molecular mechanics energy values and the experimental *J* values (see below).

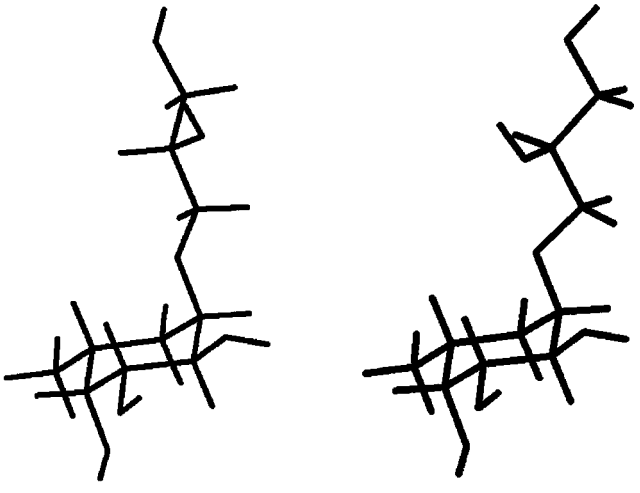

Figure 2. Simplified views of the global (left, *exo*-anomeric) and local (right, non *exo*-anomeric) low-energy minima obtained by MM3* calculations for compound **3**

NMR Studies

The validity of the predictions obtained by the molecular mechanics calculations was tested using NMR measurements, especially NOE and *J* values. In the first step, the assignment of resonances was made through a combination of COSY, HSQC and TOCSY experiments at 500 MHz. The results are shown in Table 3. The unambiguous assignment of the (pro-*RS*) hydrogen atoms at position 1′ of the lateral chains was performed by NOE/*J* analysis, using an approach similar to that described.[20]

Regarding the conformation of the lateral chain, the expected couplings were calculated from the molecular mechanics based conformational distribution, using the Altona modification of the Karplus equation.[21] In particular, the expected *J* values were calculated for each conformer, weighted according to its particular population and averaged. This produced, in all cases, a satisfactory agreement with the experimental values for Ψ/ω1/ω2. Indeed, the discrepancies between the experimental couplings (Table 3) and those estimated by the MM3* programme were smaller than 1 Hz for **1** and **3**, and less than 1.5 Hz for **2** and **4**. Care should be taken when considering the molecular mechanics based conformational distributions around C-5−C-6 and related hydroxymethyl torsions of saccharides, since it has been shown that in many cases incorrect populations may be obtained, depending on the force field used.[22] Nevertheless, in this case, the MM3* values seem to reproduce correctly the conformational behaviour around these torsions, always taking into account the important flexibility of the lateral chain, deduced from both MM-MD and NMR, especially for the C2′−C3′ torsion of the lateral chain.

The key conformational information concerning the Φ angle was obtained from NOE experiments. Close inspection of 3D models for the basic *exo*-anomeric and non-*exo*-anomeric conformations around this linkage indicated that there were exclusive[23] interresidue NOEs that should characterise both conformations unequivocally. Thus, 2D-NOESY and 1D-DPFGSE NOESY[24] spectra were acquired. The experimental NOEs (Figure 3 and Figure 4) are given in Table 4.

The *exo*-anomeric conformation around Φ is characterised by short H-1−H-1′*R* distances of 2.4 Å. In contrast, the H-1−H-1′*S* distance is 3.1 Å. The situation is reversed for the non-*exo*-anomeric orientation. In this case, the H-1−H-1′*S* distance is 2.4 Å, while the H-1−H-1′*R* distance is now 3.1 Å. In addition, there are short distances between H-5 and H-1′*S* of **1−4** and between H-5a^{eq} and H-1′*S* (of **3** and **4**), but only for the *exo*-anomeric conformations. Therefore, the presence of *exo*-anomeric conformers can be detected definitely by focussing on the existence of the H-5−H-1′*S* NOEs. Indeed, this is the case for all compounds **1−4**. The H-5a^{eq}−H-1′*S* NOE is also seen for **3** and **4**. Therefore, these data indicate that, as expected, the *exo*-anomeric conformers are present in solution. Unfortunately, there are no exclusive NOEs for the non-*exo*-anomeric conformers, since the H-1−H-1′*S* NOE (with an in-

Table 3. ^{1}H NMR chemical shifts (δ) and coupling constants (J [Hz]) for **1**−**4** in water at 300 K; DSS is used as external reference

1				**2**			
Proton	δ, multiplicity	$J_{H,H}$	[Hz]	Proton	δ, multiplicity	$J_{H,H}$	[Hz]
H-1	4.90, d	$J_{1,2}$	3.6	H-1	4.90, d	$J_{1,2}$	3.6
H-2	3.79, dd	$J_{2,3}$	10.5	H-2	3.80−3.70, m	$J_{2,3}$	10.0
H-3	3.88, dd	$J_{3,4}$	3.0	H-3	3.88, dd	$J_{3,4}$	3.5
H-4	3.81, d			H-4	3.80−3.70, m		
H-5	4.06, q	$J_{5,6}$	6.5	H-5	4.08, q	$J_{5,6}$	6.5
H-6	0.95, d	$J_{1'R,1'S}$	10.5	H-6	0.95, d	$J_{1'R,1'S}$	10.2
H-1′*R*	3.55, dd	$J_{1'R,2'}$	4.0	H-1′*R*	3.46, dd	$J_{1'R,2'}$	7.2
H-1′*S*	3.72, dd	$J_{1'S,2'}$	5.7	H-1′*S*	3.77, dd	$J_{1'S,2'}$	4.0
H-2′	3.94, dddd	$J_{2',3'a}$	6.5	H-2′	3.93, dddd	$J_{2',3'a}$	6.2
H-3′a	3.62, dd	$J_{3'a,3'b}$	11.5	H-3′a	3.58, dd	$J_{3'a,3'b}$	11.7
H-3′b	3.67, dd	$J_{2',3'b}$	6.5	H-3′b	3.66, dd	$J_{2',3'b}$	4.5
3				**4**			
Proton	δ, multiplicity	$J_{H,H}$	[Hz]	Proton	δ, multiplicity	$J_{H,H}$	[Hz]
H-1	3.78−3.74, m	−[a]		H-1	3.79−3.74, m	−[a]	
H-2	3.78−3.74, m	−[a]		H-2	3.79−3.74, m	−[a]	
H-3	3.70, d	$J_{2,3}$	3.5	H-3	3.65, d	$J_{2,3}$	4.0
H-4	3.85, m	$J_{5,6}$	6.8	H-4	3.84, m	$J_{5,6}$	6.8
H-5	1.98−1.90, m	$J_{5,5a}{}^{eq}$	2.6	H-5	1.98−1.90, m	$J_{5,5a}{}^{eq}$	2.2
H-5a^{ax}	1.40, td	$J_{5,5a}{}^{ax}$	14.7	H-5a^{ax}	1.40, t	$J_{5,5a}{}^{ax}$	14.7
H-5a^{eq}	1.80, dt	$J_{5a}{}^{eq},{}_{5a}{}^{ax}$	14.6	H-5a^{eq}	1.80, dt	$J_{5a}{}^{eq},{}_{5a}{}^{ax}$	14.7
H-6	0.95, d	$J_{1'R,1'S}$	10.2	H-6	0.95, d	$J_{1'R,1'S}$	10.2
H-1′*R*	3.49, dd	$J_{1'R,2'}$	4.0	H-1′*R*	3.40, dd	$J_{1'R,2'}$	6.7
H-1′*S*	3.66, dd	$J_{1'S,2'}$	5.7	H-1′*S*	3.69, dd	$J_{1'S,2'}$	4.5
H-2′	3.89, dddd	$J_{2',3'a}$	4.5	H-2′	3.88, dddd	$J_{2',3'a}$	6.0
H-3′a	3.60, dd	$J_{3'a,3'b}$	11.7	H-3′a	3.69, dd	$J_{3'a,3'b}$	10.5
H-3′b	3.66, dd	$J_{2',3'b}$	6.5	H-3′b	3.56, dd	$J_{2',3'b}$	4.0

[a] Overlapping.

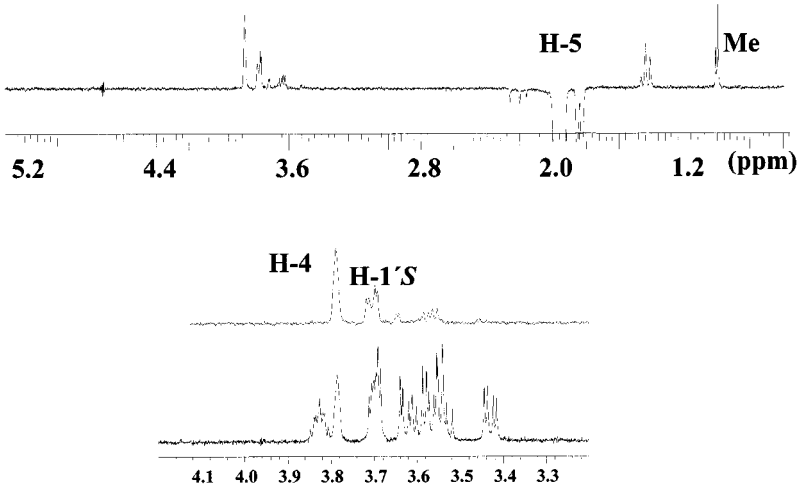

Figure 3. 1D-DPFGNOESY spectrum of **3** at 500 MHz, 303 K, D_2O, mixing time, 600 ms; a superimposition of a section of this spectrum with the regular 1D counterpart is also given

terproton distance of 2.4 Å, for pure non-*exo* forms) should also give medium-weak NOEs for the *exo* rotamers (3.1 Å). However, since the observed NOEs are averaged among all the rotamers present in solution, it can be deduced, from the interproton distances mentioned, that the presence of unique *exo*-anomeric forms should also provide large H-1−H1′*R*/H-1−H1′*S* NOE ratios. On the other hand, the presence of unique non *exo*-anomeric conformers should give rise to opposite data: large H-1−H-1′*S*/H-1−H-1′*R* NOE ratios. The presence of a 1:1 equilibrium should also correspond approximately to a H-1−H-1′*R*/H-1−H-1′*S* NOE ratio close to unity. With this reasoning, it can be observed that the experimental H-1−H-1′*R*/H-1−H-1′*S* NOE ratio is experimentally higher than 3 for the glycosides, while significantly smaller − less than 2 − for the carba analogues. This observation seems to indicate the presence of equilibria for the carba mimetics.

In an attempt to obtain more quantitative information, the deduced NOEs from the molecular mechanics ensemble average distances were compared to those measured experi-

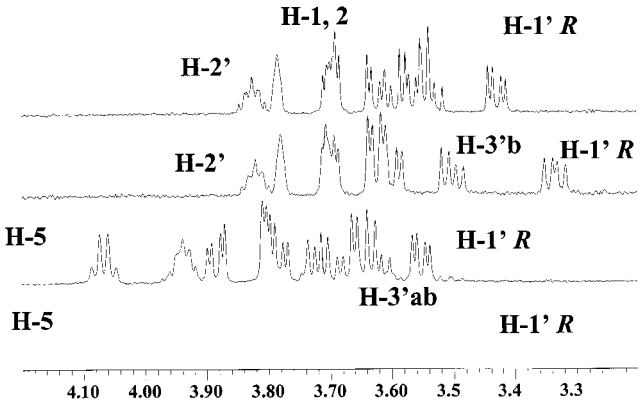

Figure 4. Superimposition of 1D-DPFGNOESY spectrum of **3**, the same spectral section for all the compounds (from bottom to top: **2**, **1**, **4**, **3**)

Thus, the molecular mechanics and NMR results allowed us to demonstrate subtly, but measurably, different conformational behaviour around the *exo*-anomeric Φ angle of the glycosides relative to their glycomimetics. For glycosides **1**−**2**, the unique conformer around Φ is centred in the *exo*-anomeric region.[27] For mimetics **3**−**4**, however, although the *exo*-anomeric conformer is also predominant, the participation of conformers with non-*exo*-anomeric orientations around Φ has been demonstrated. Since there are essentially no variations in bond lengths and angles within the glycosidic linkages of these molecules, the observed variations should be accountable for by the stereoelectronic stabilization due to the *exo*-anomeric effect in **1**−**2**. The *exo*-anomeric preference also found in the carba analogues, with no acetal-type of linkage, should mainly be due to steric effects, probably 1,3-type interactions.[5,28] In fact, for the regular $^1C_4$(**L**) chairs of the fuco series, there is, when the non-*exo*-anomeric (non-*exo*) conformation is considered, a 1,3-type interaction between the equatorially substituted C-2, as in **1**−**4,** and the aglycon (Figure 5). Such steric interactions are not present for the *exo*-anomeric (*exo*) and the *anti* conformations. Therefore, this interaction is probably the origin of the strong preference for the *exo*-anomeric orientation in **1**−**4**. The found *exo*/non-*exo* rotamer ratios of 80:20 in **3** and **4** suggest that the free energy difference corresponding to the 1,3-type interaction is about 1 kcal/mol.[5,28] For glycosides such as **1**−**2**, the stereoelectronic effect will additionally be superimposed, with subsequent further stabilization of the *exo*-anomeric orientation, thus providing the explanation for the effectively unique conformation around the Φ angle in the natural compounds.[29]

Table 4. Comparison between the experimental NOEs (1D-DPFGNOE) measured for **1**−**4** and those estimated from the probability distribution, using a full relaxation matrix approach, and a 50 ps correlation time; the correlation time was chosen to match H1/H2 of Fuc

	1		**2**		**3**		**4**	
Proton pair	Exp.	MM3*	Exp.	MM3*	Exp.	MM3*	Exp.	MM3*
H-1−H-2[a]	6.0	6.0	8.0	7.6	−[b]	7.0	7.2	6.9
H-1−H-1′*R*	4.6	9.1	4.6	11.4	3.5	6.9	4.3	7.2
H-1−H-1′*S*	1.4	1.4	1.3	2.2	1.8	1.6	−[b]	2.4
H-5−H-1′*S*	1.8	6.2	3.3	7.6	2.4	1.7	1.4	1.6
H-5a^{eq}−H-1′*R*	−[c]	−[c]	−[c]	−[c]	1.2	0.5	1.3	0.6
H-5a^{eq}−H-1′*S*	−[c]	−[c]	−[c]	−[c]	5.6	10.7	5.5	9.1
H-1′*R*−H-2	3.2	0.8	1.6	4.4	3.5	3.7	2.2	1.3

[a] 300 K and 500 MHz. 750 ms, mixing time. − [b] Overlapping. − [c] Not applicable.

mentally, using a full relaxation matrix approach. However, it was observed in all cases that, for the correlation times that fitted the intraresidue Fuc H-1/H-2 NOE, the calculated NOEs for proton pairs involving the glycerol chain were much smaller than those observed experimentally. This fact conclusively proves that the glycerol chains undergo additional internal motions that markedly reduced the NOE values.[25] Since, for a molecule of this size, the correlation times for the global and internal motion correlation times are probably of the same order of magnitude, a more quantitative analysis is precluded.[26] Nevertheless, if it is assumed that the effective correlation times for the H-1−H-1′*R* and H-1−H-1′*S* proton pairs of the glycosides (**1** and **2**) and the carba analogues (**3** and **4**) are similar, the calculations indicate that, for unique *exo*-anomeric forms, the H-1−H-1′*R*/H-1−H-1′*S* NOE ratio should be between 4 and 5, while the presence of a 20% population of non *exo*-anomeric conformers around Φ should decrease this ratio to about 1.9, in agreement with those figures deduced experimentally. Therefore, according to these experiments, the presence of non-*exo*-anomeric conformers in the glycosides is negligible, while those for glycomimetics are probably around 20%. Nevertheless, it should also be stated that, as commented by Neuhaus and Williamson,[25] "*the ability to fit NOE data using predicted conformations cannot be taken to mean that those conformations are necessarily those that are present; other choices might well fit the NOE data also*".

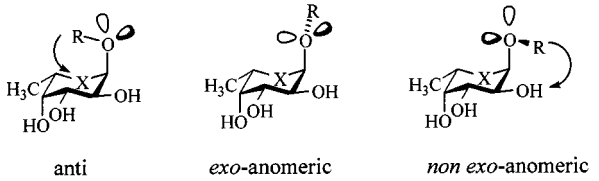

Figure 5. Schematic representation of the three possible staggered conformations around Φ of α-L-fucopyranosides; the corresponding 1,3-*syn*-diaxial-type interactions are highlighted; the *exo*-anomeric *syn* orientation of the aglycon is free of 1,3-*syn*-diaxial interactions with OH-2; from left to right, *anti*, *exo*-anomeric, non-*exo*-anomeric conformations

The Conformations of 1 and 3 when Bound to *Aurelia Aurantia Agglutinnin* (AAA)

The binding of glycoside **1** and its mimetic **3** to a well-known fucose-binding lectin, namely *Aurelia Aurantia Agglutinnin*, was followed by NMR, using regular 1D and TR-NOE experiments.[30,31] The observed linewidths of the NMR signals in both ligands after addition of the protein

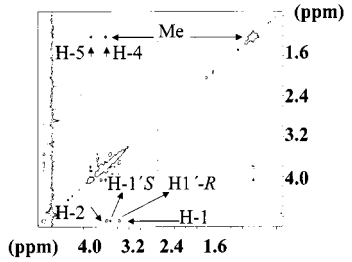

Figure 6. Partial sections of TR-NOESY spectra of **1** at 500 MHz, 303 K, D_2O, mixing time 200 ms; cross peaks corresponding to the *exo*-anomeric *syn* orientation of the aglycon are shown

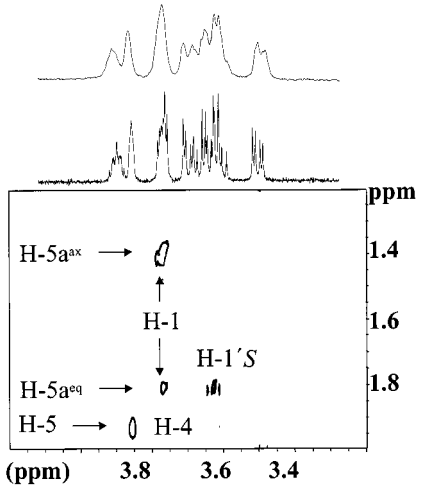

Figure 7. Partial sections of TR-NOESY spectra of **3** at 500 MHz, 303 K, D_2O, mixing time 200 ms; the variation of linewidths upon addition of AAA lectin to the NMR tube is also shown in the top trace for **3**; cross peaks corresponding to the *exo*-anomeric *syn* orientation of the aglycon are shown

were similar (Figure 6 and 7), indicating that the protein is able to recognize the fucosyl and the carbafucosyl compounds with similar affinities. In addition, TR-NOE experiments recorded for a 62:1 ligand/lectin molar ratio provided negative cross peaks, thus indicating binding of both compounds to AAA. In both cases, cross peaks exclusive to the *exo*-anomeric conformation − namely H-5−H-1′*S* for **1** and **3**, and H-5a^{eq}−H-1′*R* for **3** − were observed, indicating for both compounds the binding in solution of the major conformation around Φ (Figure 6 and 7).

The binding of the local minimum of **3**, the non-*exo* conformer, could not be proven, due partly to the much higher overlapping induced by the line broadening, and also to the much higher error in the integrals of the cross peaks, thus precluding even a semiquantitative analysis of the H1−H1′S/H1−H1′R NOE ratios. Nevertheless, the unambiguous detection of binding of the *exo*-anomeric conformation (NOE H-5a^{eq}−H-1′*R*) of **3** to AAA allowed us to demonstrate that the carbafucosyl compounds are reasonable glycomimetics of the natural analogues for both the free and the bound states of AAA. Indeed, recent results from our laboratories have demonstrated that these and other carbafucosyl analogues are able to inhibit α-fucosidase within the mM range.[32]

Conclusions

The results presented here clearly show that the Φ glycosidic linkages of carbasugars are more flexible than those of the natural glycosides, as determined by NMR and molecular mechanics calculations. The obtained results, along with those previously found for other glycomimetics, are relevant for drug design. The flexibility of these mimetics may pose a limitation to their use as therapeutic agents; an entropy penalty has to be paid and minima other than the global minimum might be bound by biological receptors.[33] Nevertheless, the small energy barriers between the different energy regions also allow that the global minimum conformation of the glycoside may be bound by the binding site of proteins without a major energy conflict. In addition, these compounds may be excellent probes for study of the combining sites of proteins and enzymes and they may also serve as test compounds to compare conformational properties of oligosaccharides.[34]

Experimental Section

Compounds: Tosylates **14** and **15** were purchased from Aldrich Co.

D-*glycero*-2,3-Dihydroxy-2,3-*O*-isopropylidenepropyl 3,4,6-Tri-*O*-benzyl-α-L-fucopyranoside (9): A solution of ethyl 3,4,6-tri-*O*-benzyl-1-thio-α-L-fucopyranoside[35] (**5**, 100 mg, 0.209 mmol) in CH_2Cl_2 (1.5 mL) was treated with Br_2 (11 μL, 0.214 mmol) over 2 h at 0°C. After this time, the solvent was evaporated and coevaporated with toluene (3 × 5 mL). The residue was dissolved in CH_2Cl_2 (0.4 mL) and added to a mixture of **7** (37 mg, 0.280 mmol), Bu_4NBr (90 mg, 0.280 mmol) and 4 Å molecular sieves (300 mg) in DMF (2.5 mL). The reaction was allowed to proceed at room temperature for 18 h, and the mixture was then treated with EtOH (2 mL) and left for 1 h. It was then filtered through a pad of Celite, diluted with CH_2Cl_2 (10 mL) and washed with sat. $NaHCO_3$ (2 × 10 mL) and H_2O (2 × 10 mL). The organic phase was dried (Na_2SO_4) and concentrated. The residue was purified by FC (hexane/EtOAc, 10:1→5:1→3:1) to give **9** (60 mg, 39%). − $[\alpha]_D$ = − 27.43 (*c* = 1.2, $CHCl_3$). − ^{1}H NMR (200 MHz, $CDCl_3$): δ = 7.44−7.23 (m, 15 H), 5.00 (d, *J* = 11.6 Hz, 1 H), 4.83 (d, *J* = 10.7 Hz, 1 H), 4.81 (d, *J* = 3.2 Hz, 1 H), 4.75 (d, *J* = 11.9 Hz, 1 H), 4.68 (d, *J* = 12.1 Hz, 1 Hz), 4.67 (d, *J* = 11.5 Hz, 1 H), 4.34 (q, *J* = 6.0 Hz, 1 H), 4.12−3.92 (m, 4 H), 3.78 (dd, *J* = 5.7 Hz, *J* = 8.3 Hz, 1 H), 3.76−3.66 (m, 2 H), 3.45 (dd, *J* = 5.9 Hz, *J* = 10.3 Hz, 1 H), 1.42 (s, 3 H), 1.37 (s, 3 H), 1.11 (d, 3 H, *J* = 6.5 Hz). − ^{13}C NMR (50 MHz, $CDCl_3$): δ = 138.9, 138.6, 138.5, 128.3, 128.3, 128.3, 128.2, 128.2, 128.1, 127.8, 127.5, 127.5, 127.4, 127.3, 109.3, 97.9, 79.2, 78.6, 77.5, 76.3, 74.3, 66.2, 74.8, 73.2, 73.1, 69.2, 66.9, 26.8, 25.4, 16.5. − $C_{25}H_{38}O_9$ (482.57): calcd. C 72.23, H 7.35; found C 72.40, H 7.65.

L-*glycero*-2,3-Dihydroxy-2,3-*O*-isopropylidenepropyl 3,4,6-Tri-*O*-benzyl-α-L-fucopyranoside (10): This compound was prepared by the same procedure as described for **9**, using alcohol **8** as the nucleophile. The residue was purified by FC (hexane/EtOAc, 10:1→5:1→3:1) to give **10** (47%). − $[\alpha]_D$ = − 43.2 (*c* = 1.4, $CHCl_3$). − ^{1}H NMR (300 MHz, $CDCl_3$): δ = 7.34−7.24 (m, 15 H), 4.94 (d, *J* = 11.6 Hz, 1 H), 4.83 (d, *J* = 11.7 Hz, 1 H), 4.82 (d, *J* = 3.7 Hz, 1 H), 4.77 (d, *J* = 12.0 Hz, 1 H), 4.69 (d, *J* = 11.8 Hz, 1 H), 4.64 (d, *J* = 8.4 Hz, 1 H), 4.61 (d, *J* = 7.9 Hz, 1 H), 4.29 (q, *J* = 6.0 Hz, 1 H), 4.01 (dd, *J* = 6.4 Hz, *J* = 9.1 Hz, 1 H), 3.99 (dt, *J* = 3.9 Hz, *J* = 9.9 Hz, 1 H), 3.88 (dd, *J* = 3.0 Hz, *J* = 10.1 Hz, 1 H), 3.83 (c, *J* = 6.0 Hz, 1 H), 3.70 (dd, *J* = 6.3 Hz, *J* = 8.2 Hz, 1 H), 3.61 (d, *J* = 2.9 Hz, 1 H), 3.54 (dd, *J* = 3.3 Hz, *J* = 5.6 Hz, 2 H), 1.36 (s, 3 H), 1.32 (s, 3 H), 1.07 (d, *J* = 6.6 Hz, 3 H). − ^{13}C NMR (50 MHz, $CDCl_3$): δ = 138.8, 138.6, 138.4, 128.4, 128.3, 128.2 (2C), 128.1, 127.8, 127.5, 127.3, 109.2, 98.0, 79.1, 77.6, 76.4, 74.7, 74.8, 73.2, 73.1, 68.9, 66.9, 66.4, 26.6, 25.3, 16.5. − $C_{25}H_{38}O_9$ (482.57): calcd. C 72.23, H 7.35; found C 71.98, H 7.21.

D-*glycero*-2,3-Dihydroxypropyl α-L-Fucopyranoside (1): A solution of **9** (40 mg, 0.073 mmol) and CF_3COOH (3 μL, 0.036 mmol) in MeOH (1 mL) was hydrogenated in the presence of 10% Pd/C (30 mg, 0.030 mmol) at room temperature over 24 h. The mixture was diluted with MeOH (5 mL), filtered through a pad of Celite and concentrated. The residue was purified by FC (CH_2Cl_2/MeOH, 10:1→5:1) to give **1** (17 mg, 99%), m.p. 123−126 °C. − $[\alpha]_D$ = −134.5 (*c* = 0.7, $CHCl_3$). − ^{1}H NMR (500 MHz, D_2O): δ = 4.90 (d, *J* = 3.6 Hz, 1 H), 4.06 (q, *J* = 6.5 Hz, 1 H), 3.94 (dddd, *J* = 4.0 Hz, *J* = 4.7 Hz, *J* = 5.7 Hz, *J* = 6.5 Hz, 1 H), 3.88 (dd, *J* = 3.5 Hz, *J* = 10.5 Hz, 1 H), 3.81 (d, *J* = 3.0 Hz, 1 H), 3.79 (dd, *J* = 3.7 Hz, *J* = 10.2 Hz, 1 H), 3.72 (dd, *J* = 5.7 Hz, *J* = 10.7 Hz, 1 H), 3.67 (dd, *J* = 4.7 Hz, *J* = 12.0 Hz, 1 H), 3.62 (dd, *J* = 6.5 Hz, *J* = 11.5 Hz, 1 H), 3.55 (dd, *J* = 4.0 Hz, *J* = 10.5 Hz, 1 H), 0.95 (d, *J* = 6.5 Hz, 3 H). − ^{13}C NMR (75 MHz, D_2O): δ = 91.3, 73.1, 71.7, 70.8, 69.8, 69.4, 68.0, 63.7, 16.5. − $C_9H_{18}O_7 \cdot 1/2H_2O$ (247.24): calcd. C 43.72, H 7.69; found C 43.78, H 7.62.

L-*glycero*-2,3-Dihydroxypropyl α-L-Fucopyranoside (2): This compound was prepared from **10** by the method described above for **1**. Purification by FC (CH_2Cl_2/MeOH, 10:1→5:1) gave **2** (17 mg, 99%), m.p. 101−103 °C. − $[\alpha]_D$ = − 124.8 (*c* = 0.4, $CHCl_3$). − ^{1}H NMR (500 MHz, D_2O): δ = 4.90 (d, *J* = 3.6 Hz, 1 H), 4.08 (q, *J* = 6.5 Hz, 1 H), 3.93 (dddd, *J* = 4.0 Hz, *J* = 4.5 Hz, *J* = 6.2 Hz, *J* = 7.2 Hz, 1 H), 3.88 (dd, *J* = 3.5 Hz, *J* = 10.0 Hz, 1 H), 3.80−3.70 (m, 3 H), 3.66 (dd, *J* = 4.5 Hz, *J* = 11.5 Hz, 1 H), 3.58 (dd, *J* = 6.2 Hz, *J* = 11.7 Hz, 1 H), 3.46 (dd, *J* = 7.2 Hz, *J* = 10.2 Hz, 1 H), 0.95 (d, *J* = 6.5 Hz, 3 H). − ^{13}C NMR (50 MHz, D_2O): δ = 100.1, 73.1, 72.0, 71.9, 70.3, 69.5, 67.9, 63.8, 16.5. − $C_9H_{18}O_7.H_2O$ (256.25): calcd. C 43.72, H 7.69; found C 43.75, H 7.96.

D-*glycero*-2,3-Dihydroxy-2,3-*O*-isopropylidenepropyl 4-*O*-Benzyl-2,3-di-*O*-(2,3-dimethoxybutane-2,3-diyl)-5a-carba-α-L-fucopyranoside (12): A solution of **11** (75 mg, 0.2 mmol) in DMF (2 mL) was treated with 95% NaH (21 mg, 0.89 mmol) at room temperature. After 20 min, a solution of Bu_4NI (82 mg, 0.22 mmol) and D-*glycero*-2,3-dihydroxy-2,3-*O*-isopropylidenepropyl *p*-toluenesulfonate (**14**, 190 mg, 0.666 mmol) in DMF (0.9 mL) was added and the reaction was allowed to proceed at 90 °C for 8 h. The reaction mixture was cooled to room temperature, and additional 95% NaH (21 mg, 0.888 mmol) was added. It was then heated to 90 °C for 20 h. After this period, the reaction mixture was cooled and quenched with MeOH (1 mL). The solvents were evaporated and the residue was purified by FC (hexane/EtOAc, 20:1→10:1→5:1) to give **12** (70 mg, 70%). − $[\alpha]_D$ = + 101.2 (*c* = 1.0, $CHCl_3$). − ^{1}H NMR (200 MHz, $CDCl_3$): δ = 7.49−7.30 (m, 5 H), 5.01 (d, *J* = 11.1 Hz, 1 H), 4.52 (d, *J* = 11.2 Hz, 1 H), 4.38−4.24 (m, 1 H), 4.12−3.94 (m, 4 H), 3.79 (dd, *J* = 3.7 Hz, *J* = 10.7 Hz, 1 H), 3.66−3.56 (m, 3 H), 3.24 (s, 6 H), 2.11−1.91 (m, 1 H), 1.62−1.54 (m, 2 H), 1.43 (s, 3 H), 1.38 (s, 3 H), 1.29 (s, 3 H), 1.28 (s, 3 H), 0.96 (d, *J* = 6.7 Hz, 3 H). − ^{13}C NMR (50 MHz, $CDCl_3$): δ = 139.9, 128.1, 127.9, 127.1, 109.0, 99.0, 98.9, 79.9, 76.4, 75.0, 74.3, 72.1, 70.0, 69.2, 67.2, 47.6, 47.5, 35.2, 30.3, 26.7, 25.5, 17.8, 17.7, 17.3.

L-*glycero*-2,3-Dihydroxy-2,3-*O*-isopropylidenepropyl 4-*O*-Benzyl-2,3-di-*O*-(2,3-dimethoxybutane-2,3-diyl)-5a-carba-α-L-fucopyranoside (13): This compound was prepared by the same procedure as for **12**. Purification by FC (hexane/EtOAc, 20:1→10:1→5:1) gave **13** (73%). − ^{1}H NMR (300 MHz, $CDCl_3$): δ = 7.48−7.28 (m, 5 H), 5.00 (d, *J* = 11.0 Hz, 1 H), 4.51 (d, *J* = 11.2 Hz, 1 H), 4.35−4.28 (m, 1 H), 4.09−3.94 (m, 4 H), 3.81 (dd, *J* = 3.7 Hz, *J* = 10.7 Hz, 1 H), 3.66−3.56 (m, 3 H), 3.23 (s, 6 H), 2.05−1.95 (m, 1 H), 1.59−1.51 (m, 2 H), 1.42 (s, 3 H), 1.38 (s, 3 H), 1.28 (s, 3 H), 1.27 (s, 3 H), 0.95 (d, *J* = 6.8 Hz, 3 H). − ^{13}C NMR (50 MHz, $CDCl_3$): δ = 140.0, 128.1, 120.1, 127.1, 108.9, 99.0, 98.9, 74.9, 74.3, 72.9, 70.8, 70.1, 69.4, 68.9, 66.8, 47.5, 33.2, 30.4, 26.6, 25.7, 17.8, 17.4.

D-*glycero*-2,3-Dihydroxy-propyl 5a-Carba-α-L-fucopyranoside (3): A solution of **12** (80 mg, 0.155 mmol) in AcOH/H_2O (2:1, 1 mL) was stirred at 100 °C for 2 h, and the solvents were then evaporated. The residue was purified by FC (CH_2Cl_2/MeOH, 20:1) to give D-*glycero*-2,3-dihydroxypropyl 4-*O*-benzyl-5a-carba-α-L-fucopyranoside (40 mg, 69%): − ^{1}H NMR (200 MHz, CD_3OD): δ = 7.40−7.23 (m, 5 H), 4.95 (d, *J* = 11.4 Hz, 1 H), 4.56 (d, *J* = 11.4 Hz, 1 H), 3.81−3.55 (m, 7 H), 3.44 (dd, *J* = 4.1 Hz, *J* = 9.9 Hz, 2 H), 2.05−1.85 (m, 1 H), 1.70 (dt, *J* = 3.7 Hz, *J* = 12.3 Hz, 1 H), 1.51 (td, *J* = 2.0 Hz, *J* = 12.6 Hz, 1 H), 0.96 (d, *J* = 6.8 Hz, 3 H). −^{13}C NMR (50 MHz, CD_3OD): δ = 141.1, 129.4, 129.0, 128.6, 84.4, 80.1, 76.8, 75.0, 73.4, 72.5, 71.8, 64.9, 31.9, 31.3, 18.2. − This compound was dissolved in MeOH (0.5 mL), and 10% Pd/C (20 mg, 0.020 mmol) was added. The reaction mixture was hydrogenated at room temperature for 2 h, and then filtered and concentrated to give **3** (22 mg, 76%). − $[\alpha]_D$ = − 65.1 (*c* = 0.4, $CHCl_3$). − ^{1}H NMR (500 MHz, D_2O): δ = 3.89 (dddd, *J* = 4.0 Hz, *J* = 4.5 Hz, *J* = 5.7 Hz, *J* = 6.5 Hz, 1 H), 3.85 (m, 1 H), 3.78−3.74 (m, 2 H), 3.69 (d, *J* = 3.5 Hz, 1 H), 3.66 (dd, *J* = 4.5 Hz, *J* = 11.7 Hz, 1 H), 3.62 (dd, *J* = 5.7 Hz, *J* = 10.2 Hz, 1 H), 3.60 (dd, *J* = 6.5 Hz, 11.0 Hz, 1 H), 3.49 (dd, *J* = 4.0 Hz, *J* = 11.0 Hz, 1 H), 1.99−1.89 (m, 1 H), 1.80 (dt, *J* = 2.6 Hz, *J* = 14.6 Hz, 1 H), 1.40 (td, *J* = 1.9 Hz, *J* = 14.7 Hz, 1 H), 0.95 (d, *J* = 6.8 Hz, 3 H). − ^{13}C NMR (75 MHz, D_2O): δ = 78.3, 74.2, 71.9, 71.1, 71.0, 69.8, 62.9, 28.9, 28.8, 16.5. − $C_{10}H_{20}O_6$ (236.26): calcd. C 64.98, H 8.39; found C 65.03, H 8.25.

L-*glycero*-2,3-Dihydroxypropyl 5a-Carba-α-L-fucopyranoside (4): This compound was prepared from **13** by the procedure described above for the preparation of **3**. Compound **4** was obtained as a syrup (58%). L-*glycero*-2,3-Dihydroxypropyl 4-*O*-benzyl-5a-carba-α-L-fucopyranoside: − ^{1}H NMR (200 MHz, CD_3OD): δ = 7.44−7.23 (m, 5 H), 4.96 (d, *J* = 11.4 Hz, 1 H), 4.56 (d, *J* = 11.4 Hz, 1 H), 3.86−3.55 (m, 7 H), 3.38−3.26 (m, 2 H), 2.04−1.88 (m, 1 H), 1.71 (dt, *J* = 3.6 Hz, *J* = 12.2 Hz, 1 H), 1.50 (td, *J* = 2.1 Hz, *J* = 12.1 Hz, 1 H), 0.95 (d, *J* = 7 Hz, 3 H). − ^{13}C NMR (50 MHz, CD_3OD): δ = 141.1, 129.4, 129.0, 128.6, 84.3, 80.5, 76.9, 74.7, 73.5, 73.0, 72.7, 64.5, 31.8, 31.2, 18.2. − **4:** − $[\alpha]_D$ = − 42.3 (*c* = 0.6, $CHCl_3$). − ^{1}H NMR (500 MHz, D_2O): δ = (dddd, *J* = 4.0 Hz, *J* = 4.5 Hz, *J* = 6.0 Hz, *J* = 6.7 Hz, 1 H), 3.84 (m, 1 H), 3.75−3.77 (m, 2 H), 3.69 (dd, *J* = 3.5 Hz, *J* = 10.5 Hz, 2 H), 3.65

(d, J = 4.0 Hz, 1 H), 3.56 (dd, J = 6.0 Hz, J = 11.5 Hz, 1 H), 3.40 (dd, J = 6.5 Hz, J = 8.2 Hz, 1 H), 1.90−1.98 (m, 1 H), 1.80 (dt, J = 2.2 Hz, J = 14.7 Hz, 1 H), 1.40 (t, J = 14.7 Hz, 1 H), 0.95 (d, J = 6.8 Hz, 3 H). − ^{13}C NMR (75 MHz, D_2O): δ = 73.88, 67.19, 66.46, 66.47, 65.52, 58.14, 24.27, 24.02, 11.79 (C-6). − $C_{10}H_{20}O_6$ (236.26): calcd. C 64.98, H 8.39; found C 65.11, H 8.31.

Molecular Mechanics and Dynamics Calculations: Molecular mechanics and dynamics calculations were performed using the MM3* force field as implemented in MACROMODEL 4.5.[36] Glycosidic torsion angles are defined as follows: Φ as H1′−C1′−O−C1, Ψ as C1′−O−C1−C2, ω1 as O−C1−C2−C3, and ω2 as C1−C2−C3−O3. The results are shown in Table 1. For Ψ and ω, the rotamers are defined as g+ (60°), g− (−60°), and *anti* (180°), while for Φ, conformers in conformity with the *exo*-anomeric orientation (Φ ca. +60) and in disagreement (Φ ca. −60) are denoted as *exo* and non-*exo*, respectively. A dielectric constant ε = 80 and the GB/SA continuum solvent model were performed; 81 initial geometries were considered for each compound, by combining the staggered orientations for Φ, Ψ and ω. Neither the non-*exo* and *anti* orientations of the glycosides **1** and **2,** nor the *anti* conformers of the mimetics **3** and **4** were local minima, and they converged to their corresponding *exo* conformers. From the energy values, probability distributions were calculated for each conformer, according to a Boltzmann function at 300 K. − The global energy minimum structures were used as starting geometries for molecular dynamics (MD) simulations at 300 K, with the GB/SA solvent model, and a time step of 1 fs. The equilibration period was 100 ps. After this period, structures were saved every 0.5 ps. The total simulation time was 1 ns for every run. Average distances between intraresidue and interresidue proton pairs were calculated from the dynamics simulations.[37]

NMR Spectroscopy: NMR experiments were recorded with a Varian Unity 500 spectrometer, using approximately 2 mg/mL solutions of the glycosides and carbasugars at different temperatures (299−313 K). Chemical shifts are reported in ppm, using external TMS (δ = 0) as reference. The double quantum-filtered COSY spectrum was performed with a data matrix of 256 × 1 K to digitize a spectral width of 2000 Hz; 16 scans were used, with a relaxation delay of 1 s. The 2D TOCSY experiment was performed using a data matrix of 256 × 2 K to digitize a spectral width of 2000 Hz; 4 scans were used per increment, with a relaxation delay of 2 s. MLEV 17 was used for the 100 ms isotropic mixing time. The one-bond proton−carbon correlation experiment was collected in the ^{1}H-detection mode, using the HSQC sequence and a reverse probe. A data matrix of 256 × 2 K was used to digitize a spectral width of 2000 Hz in F_2 and 10000 Hz in F_1. Four scans were used per increment, with a relaxation delay of 1 s and a delay corresponding to a J value of 145 Hz. A BIRD pulse was used to minimize the ^{12}C-bonded proton signals; ^{13}C decoupling was achieved by the WALTZ scheme. − NOESY experiments were performed with the selective 1D double pulse field gradient spin echo module,[24] using three different mixing times, namely 250, 500 and 750 ms. 2D NOESY experiments were also performed with the same mixing times, and using 256×2 K matrixes.

NOE Calculations: NOESY spectra were simulated according to a complete relaxation matrix approach, following the protocol previously described, using three different mixing times (between 250 and 750 ms). The spectra were simulated from the average distances $<r^{-6}>_{kl}$ calculated from the population distribution at 303 K. Isotropic motion and external relaxation of 0.1 s^{-1} were assumed. A τ_c of 50 ps was used to obtained the best match between experimental and calculated NOEs for the intraresidue proton pairs (Fuc H-1/H-2). All the NOE calculations were automatically performed by a custom program, available from the authors upon request.

TR-NOE Experiments: The ligand was exposed to repeated cycles of freeze-drying with D_2O, and transferred to the NMR tube to give a final concentration of 0.5 mM. TR-NOESY experiments were performed with mixing times of 200 ms and 300 ms, for a 62:1 molar ratio of ligand/lectin. In all cases, line-broadening of the sugar protons was monitored after the addition of the ligand. TR-ROESY experiments were also carried out to detect spin diffusion effects (not shown). A continuous wave spin lock pulse was used during the 250 ms mixing time. Key NOEs were shown to be direct cross peaks, since they showed different signs to diagonal peaks.

Acknowledgments

Financial support by DGICYT (Grant PB96−0833) is gratefully acknowledged. M. C. thanks CAM for a fellowship. We warmly thank Prof. T. Peters (Lübeck) for a gift of the AAA lectin and discussions.

[1] [1a] *Glycosciences: Status and Perspectives* (Eds.: H. J. Gabius, S. Gabius), Chapman & Hall, London, **1997.** − [1b] *Chemistry of C-glycosides* (Eds.: W. Levy, D. Chang), Elsevier, Cambridge, **1995**. − [1c] M. D. H. Postema, *C-Glycoside synthesis*, CRC Press, Boca Raton, **1995**. − [1d] H. Driguez, *Topics Curr. Chem.* **1997**, *187*, 85−116. − [1e] J. S. Andrews, B. M. Pinto, *Carbohydr. Res.* **1995**, *270*, 51−62. − [1f] H. Yuasa, H. Hashimoto, *Rev. Heteroatom Chem.* **1999**, *19*, 35−65.

[2] [2a] B. A. Johns, Y. T. Pan, A. D. Elbein, C. R. Johnson, *J. Am. Chem. Soc.* **1997**, *119*, 4856−4865. − [2b] H.-J. Gabius, F. Sinowatz (Eds.), "Special volume on glycosciences", *Acta Anat.* **1998**, *161*, 1−276.

[3] S. Ogawa, K. Hirai, T. Odagiri, N. Matsunaga, T. Yamazaki, A. Nakajima, *Eur. J. Org. Chem.* **1998**, *1*, 1099−1109, and references therein.

[4] M. S. Searle, D. H. Williams, *J. Am. Chem. Soc.* **1992**, *114*, 10690−10697.

[5] [5a] J. L. Asensio, F. J. Cañada, A. García, M. T. Murillo, A. Fernández-Mayoralas, B. A. Johns, J. Kozak, Z. Zhu, C. R. Johnson, J. Jiménez-Barbero, *J. Am. Chem. Soc.* **1999**, *121*, 11318−11329. − [5b] J. L. Asensio, F. J. Cañada, N. Kahn, D. A. Mootoo, J. Jiménez-Barbero, *Chem. Eur. J.* **2000**, *6*, 1035−1041.

[6] E. Montero, A. García, J. L. Asensio, K. Hirai, S. Ogawa, F. Santoyo-González, F. J. Cañada, J. Jiménez-Barbero, *Eur. J. Org. Chem.* **2000**, 1945−1952.

[7] E. Montero, M. Vallmitjana, J. A. Perez-Pons, E. Querol, J. Jiménez-Barbero, J. Cañada, *FEBS Lett.* **1998**, *421*, 243−248.

[8] J. F. Espinosa, E. Montero, A. Vian, J. L. Garcia, H. Dietrich, M. Martín-Lomas, R. R. Schmidt, A. Imberty, F. J. Cañada, J. Jiménez-Barbero, *J. Am. Chem. Soc.* **1998**, *120*, 10862−10871.

[9] [9a] J. F. Espinosa, F. J. Cañada, J. L. Asensio, H. Dietrich, M. Martín-Lomas, R. R. Schmidt, J. Jiménez-Barbero, *Angew. Chem. Int. Ed. Engl.* **1996**, *35*, 303−306. − [9b] J. F. Espinosa, F. J. Cañada, J. L. Asensio, M. Martín-Pastor, H. Dietrich, M. Martín-Lomas, R. R. Schmidt, J. Jiménez-Barbero, *J. Am. Chem. Soc.* **1996**, *118*, 10862−10871.

[10] J. L. Asensio, J. F. Espinosa, H. Dietrich, F. J. Cañada, R. R. Schmidt, M. Martín-Lomas, S. André, H. J. Gabius, J. Jiménez-Barbero, *J. Am. Chem. Soc.* **1999**, *121*, 8995−9000.

[11] R. Ravishankar, A. Surolia, M. Vijayan, S. Lim, Y. Kishi, *J. Am. Chem. Soc.* **1998**, *120*, 11297−11303.

[12] [12a] T. Peters, B. M. Pinto, *Curr. Opin. Struct. Biol.* **1996**, *6*, 710−720. − [12b] A. Imberty, *Curr. Opin. Struct. Biol.* **1997**, *7*, 617−623. − [12c] J. Jiménez-Barbero, J. L. Asensio, J. Cañada, A. Poveda, *Curr. Opin. Struct. Biol.* **1999**, *9*, 549−555.

[13] A general survey of conformation of carbohydrates and analogues is presented in: A. D. French, J. W. Brady, *Computer Modelling of Carbohydrate Molecules*, American Chemical Society, **1990**. For carbasugars, besides ref.[6], see: [13a] J. O. Duus, K. Bock, S. Ogawa, *Carbohydr. Res.* **1994**, *252*, 1−18. − [13b] J. O. Duus, J. F. Guzmán, K. Bock, S. Ogawa, F. Yokoi, *Car-*

bohydr. Res. **1991**, *209*, 51−65. − [13c] K. Bock, J. F. Guzman, S. Ogawa, *Carbohydr. Res.* **1988**, *174*, 354−359. − [13d] K. Bock, S. Ogawa, M. Orihara, *Carbohydr. Res.* **1989**, *191*, 357−363.

[14] For fucose derivatives binding to AAA, see T. Weimar, T. Peters, *Angew. Chem. Int. Ed. Engl.* **1994**, *33*, 88−91.

[15] R. U. Lemieux, K. B. Hendriks, R. V. Stick, K. James, *J. Am. Chem. Soc.* **1975**, *97*, 4056−4062.

[16] The synthesis of **11** will be described elsewhere.

[17] M. K. Dowd, P. J. Reilly, A. D. French, *Biopolymers* **1994**, *34*, 625−638.

[18] The MM3* force field was used since it has provided a satisfactory agreement between experimental and theoretical data for a variety of saccharides and carbasugars, see ref.[6] For specific cases, see ref.[18a][18a] J. F. Espinosa, H. Dietrich, M. Martín-Lomas, R. R. Schmidt, J. Jiménez-Barbero, *Tetrahedron Lett.* **1996**, *37*, 1467−1470. − [18b] M. Martín-Pastor, J. F. Espinosa, J. L. Asensio, J. Jimenez-Barbero, *Carbohydr. Res.* **1997**, *298*, 15−47.

[19] W. C. Still, A. Tempczyk, R. C. Hawley, T. Hendrickson, *J. Am. Chem. Soc.* **1990**, *112*, 6127−6128.

[20] J. F. Espinosa, M. Bruix, O. Jarreton, T. Skrydstrup, J.-M. Beau, J. Jiménez-Barbero, *Chem. Eur. J.* **1999**, *5*, 442−448.

[21] C. A. G. Haasnoot, F. A. A. M. de Leeuw, C. Altona, *Tetrahedron* **1980**, *36*, 2783−2794.

[22] S. Perez, A. Imberty, S. Engelsen, J. Gruza, K. Mazeau, J. Jimenez-Barbero, A. Poveda, J. F. Espinosa, *Carbohydr. Res.* **1998**, *314*, 141−155.

[23] J. Dabrowski, T. Kozar, H. Grosskurth, N. E. Nifant'ev, *J. Am. Chem. Soc.* **1995**, *117*, 5534−5539.

[24] K. Stott, J. Stonehouse, J. Keeler, T.-L. Hwang, A. J. Shaka, *J. Am. Chem. Soc.* **1995**, *117*, 4199−4200.

[25] D. Neuhaus and M. P. Williamson, *The Nuclear Overhauser Effect in Structural and Conformational Analysis*, VCH Publishers, New York, **1989**.

[26] G. Lipari, A. Szabo, *J. Am. Chem. Soc.* **1982**, *104*, 4546−4555.

[27] [27a] R. U. Lemieux, S. Koto, D. Voisin, *Am. Chem. Soc. Symp. Ser.* **1979**, *87*, 17−29. − [27b] G. R. J. Thatcher, *The Anomeric Effect and Associated Stereoelectronic Effects*, American Chemical Society, Washington, DC, **1993**. − [27c] I. Tvaroska, T. Bleha, *Adv. Carbohydr. Chem. Biochem.* **1989**, *47*, 45−103. − [27d] A. J. Kirby, *The Anomeric Effect and Related Stereoelectronic Effects at Oxygen*, Springer-Verlag, Heidelberg, Germany, **1983**.

[28] A. Poveda, J. L. Asensio, H. Bazin, T Polat, R. J. Lindhardt, J. Jimenez-Barbero, *Eur. J. Org. Chem.* **2000**, 1805−1813.

[29] For the occurrence of other conformations, see for example: C. Landersjo, R. Stenutz, G. Widmalm, *J. Am. Chem. Soc.* **1997**, *119*, 8695−8701.

[30] For a survey of applications of TR-NOESY to saccharide binding to proteins, see for example: A. Poveda, J. Jimenez-Barbero, *Chem. Soc. Rev.* **1998**, *27*, 133−143.

[31] For applications of TR-ROESY to saccharide binding to proteins, see for example: J. L. Asensio, J. Cañada, J. Jimenez-Barbero, *Eur. J. Biochem.* **1995**, *233*, 618−630. For potential problems in the application of TR-ROESY, see: T. Haselhorst, J. F. Espinosa, J. Jiménez-Barbero, T. Sokolowski, P. Kosma, H. Brade, L. Brade, T. Peters, *Biochemistry* **1999**, *38*, 6449−6459.

[32] Unpublished results.

[33] For different implications of conformational restriction of the ligand upon protein binding, see: [33a] D. R. Bundle, R. Alibés, S. Nilar, A. Otter, M. Warwas, P. Zhang, *J. Am. Chem. Soc.* **1998**, *120*, 5317−5318. − [33b] N. Navarre, N. Amiot, A. H. van Oijen, A. Imberty, A. Poveda, J. Jimenez-Barbero, A. Cooper, M. A. Nutley, G. J. Boons, *Chem. Eur. J.* **1999**, *5*, 2281−2294.

[34] For conformational selection in carbohydrate recognition by proteins, besides glycomimetic recognition references given in refs.[9−12], see: M. Gilleron, H.-C. Siebert, H. Kaltner, C. W. von der Lieth, T. Kozar, K. M. Halkes, E. Y. Korchagina, N. V. Bovin, H.-J. Gabius, J. F. G. Vliegenthart, *Eur. J. Biochem.* **1998**, *249*, 27−38.

[35] H. Lohn, *Carbohydr. Res.* **1985**, *53*, 105−113.

[36] The MM3* force field (N. L. Allinger, Y. H. Yuh, J. H. Lii, *J. Am. Chem. Soc.* **1989**, *111*, 8551−8558) implemented in MACROMODEL (F. Mohamadi, N. G. J. Richards, W. C. Guida, R. Liskamp, C. Caufield, G. Chang, T. Hendrickson, W. C. Still, *J. Comput. Chem.* **1990**, *11*, 440−467) differs from the regular MM3 force field in the treatment of the electrostatic term, since it uses charge−charge rather than dipole−dipole interactions.

[37] For a detailed description of conformational analysis of carbohydrates using MD simulations, see: R. J. Woods, *Curr. Opin. Struct. Biol.* **1995**, *5*, 591−598.

Received July 20, 2000
[O00375]